Journal of the Korean Society of Oceanography
Vol. 37, No. 3, pp. 000 — 000 September 2002

**INFORMATION**

# Eddy Formation Near the Izu-Ogasawara Ridge and its Link with Seasonal Adjustment of the Subtropical Gyre in the Pacific

CHIE IHARA[1], TAKASHI KAGIMOTO[2], YUKIO MASUMOTO[3] AND TOSHIO YAMAGATA[4]
[1]*Department of Earth and Planetary Science, Graduate School of Science, The University of Tokyo, Tokyo 113-0033, Japan.*
[2]*IGCR, Frontier Research System for Global Change, SEVANS North 7F, 1-2-1 Shibaura, Minato-ku, Tokyo 105-6791, Japan.*
[3,4]*Department of Earth and Planetary Science, Graduate School of Science, The University of Tokyo, Tokyo 113-0033*

Using OGCM results, we have shown that the ring-like cold baroclinic eddies associated with cyclonic circulation are shed from late summer to early fall near the Izu-Ogasawara Ridge from the Kuroshio Extension owing to baroclinic instability. On the other hand, warm baroclinic eddies are generated by the intensified western boundary current associated with the warm anomaly accumulated near the Ridge in winter, which corresponds to the basin-wide barotropic intensification of the wind-driven gyre in winter. We are successful in reproducing the behavior of those meso-scale eddies using a simple two-layer primitive equation model driven by seasonal winds associated with the positive curl. Those eddies carry barotropic seasonal signals originated in the Pacific Basin quite slowly west of the ridge; this process introduces a phase lag in the timing of the seasonal maximum transport in the Philippine Basin west of the ridge. It is demonstrated that the existence of bottom topography, baroclinicity, and nonlinearity due to advection are three necessary elements for the generation of these eddies south of Japan.

**Key words:** The kuroshio, Izu-ogasawara Ridge, Meso-scale eddies, Baroclinicity, Seasonal winds

## INTRODUCTION

The mysterious bimodal behavior of the Kuroshio path has long been one of intriguing problems for physical oceanographers. To study roles of meso-scale eddies south of Japan are now becoming a hot topic in regard to predictability of this meandering of the Kuroshio. It is a quite interesting question whether one can predict the Kuroshio meander using a general ocean circulation model assimilated with *in situ* and satellite observations. Considering that a large transport is necessary for the large meander of the Kuroshio south of Japan (Kawabe, 1995), these meso-scale eddies may trigger the meander when the condition is satisfied. Actually, Endoh and Hibiya (2001) is successful in reproducing the Kuroshio meander using a source-sink ocean model by assuming an impinging intense warm eddy south of Kyushu. According to recent observations, those eddies, either cyclones or anticyclones, propagate westward frequently in the northern Philippine Basin. Using surface velocity data measured by Acoustic Doppler Current Profilers (ADCPs) and sea surface height anomalies measured by TOPEX/POSEIDON altimeter, Ebuchi and Hanawa (2000) reported that these eddies are circular in shape with a diameter of 500 km and a time scale of 80 days. Waseda *et al*. (2000) also reported propagation of eddies south of Japan using the TOPEX/POSEIDON altimeter data. Because of the rapid evolution of supercomputers, these eddies are also simulated in high-resolution general ocean models (Miyazawa *et al*., 2000; Kagimoto, 1999). Although more and more information about the eddies is now accumulating, it is still not clear how and where the synoptic eddies are generated. Recently, Kagimoto (1999), using a high-resolution general circulation model, showed a very interesting feature on the eddy propagation as well as the eddy generation in the lon-

*Corresponding author: kagimoto@frontier.esto.or.jp

gitude-time section of transport streamfunction anomaly. Since the seasonal wind field in the North Pacific changes dramatically, the Sverdrup transport also changes in accord to the forcing field. This is clearly seen over a relatively flat bottom in the east of the Izu-Ogasawara Ridge of the Pacific Basin; there are positive streamfunction anomalies in winter and negative anomalies in summer. This is reasonable because the adjustment due to barotropic Rossby waves is accomplished within a week even for the wide Pacific Basin (Gill, 1982). However, in the smaller Philippine Basin west of the ridge, we observe that the annual signal from the east propagates slowly westward in contrast to the almost instantaneous response to the seasonal variation of winds in the Pacific Basin. As we will see later, the slow signals are due to cold eddies in summer and warm eddies in winter. These synoptic eddies are somehow generated near the ridge and, quite interestingly, the generation appears to be regulated by the seasonal march of the basin-wide adjustment processes. Therefore we study possible generation mechanisms of these eddies, taking into account the basin-wide seasonal phenomenon. In particular, we pay attention to the role of the Izu-Ogasawara Ridge. In Section 2, we analyze the data from the realistic OGCM in detail. Based on the analysis, we construct in Section 3 a simple model that captures the basic feature of the OGCM results in regard to the eddy formation linked to the seasonal march of the basin-wide response to seasonal winds. In Section 4, we discuss results from the simple model. Section 5 is devoted to summary and discussion based on the concept of the joint effect of baroclinicity and bottom relief (JEBAR).

## ANALYSIS OF GCM RESULTS

### *Data source*

The data used in the present article is from a numerical ocean model based on MOM developed at GFDL/NOAA (Pacanowski, 1996). Although the model domain covers most of the Pacific, we examine only the Kuroshio region from 120°E to 180°E and from 10°N to 40°N. The horizontal grid spacing is variable in the model. The finest grid spacing is 1/4°×1/4° in the Kuroshio region from 120°E to 180°E and 20°N to 40°N, while the coarsest grid spacing is 1/2°×1/3° east of 170°W and south of equator. There are 30 levels in the vertical, of which 10 are assigned to the upper 100 m with a spacing of 5 m in the uppermost 6 levels. Bottom topography adopted in the present model is based on the ETOPO5 dataset; it is smoothed in order to make the numerical calculation stable (Killworth, 1987). Lateral eddy viscosity and diffusivity are calculated using the formula proportional to the horizontal grid spacing as well as the total deformation rate (Smagorinsky, 1963). Vertical eddy viscosity and diffusivity are parameterized in terms of the function of Richardson number (Pacanowski and Philander, 1981). The strategy to apply the surface boundary condition to the model is almost the same as that of Rosati and Miyakoda (1988). We use, however, the NCEP/NCAR reanalysis data, and introduce the correction term into the net heat flux to relax the sea surface temperature to the observation (Smith *et al.*, 1996) in a relatively long time scale of 60 days. The surface boundary condition for the salinity is the restoring condition using the monthly mean climatology (Levitus *et al.*, 1994). The relaxation time scale is the same with that of the temperature. Near the northern and southern boundaries, the sponge layer with 3 degrees in width, in which the temperature and salinity are relaxed to the monthly mean climatology (Levitus and Boyer, 1994; Levitus *et al.*, 1994), is introduced to mitigate effects of artificial walls such as the propagation of unrealistic Kelvin wave along the northern and southern boundaries. The model is started from the annual mean temperature and salinity field with no motion (Levitus and Boyer, 1994; Levitus *et al.*, 1994) and integrated for 15 years with forcing calculated from the climatological NCEP/NCAR reanalysis data. Then the model is further integrated from January 1979 to December 1997 using daily NCEP/NCAR reanalysis data, in which the high frequency variability is filtered out with 3 days running mean. Snapshot data is stored every five days (see Kagimoto, 1999 for more details).

### *Analysis of the simulation data*

As we discussed in Introduction, the clear seasonal signal of negative (positive) streamfunction anomaly in summer (winter) in the Pacific Basin changes its character drastically west of the Izu-Ogasawara Ridge. This change is associated with formation of warm and cold eddies. Therefore we examine the process by focusing on typical events of the eddy shedding.

**Cold Eddies:** We select a typical case for formation of a cold eddy during 1984-1985. From the snapshot of the sea surface height (SSH) at this

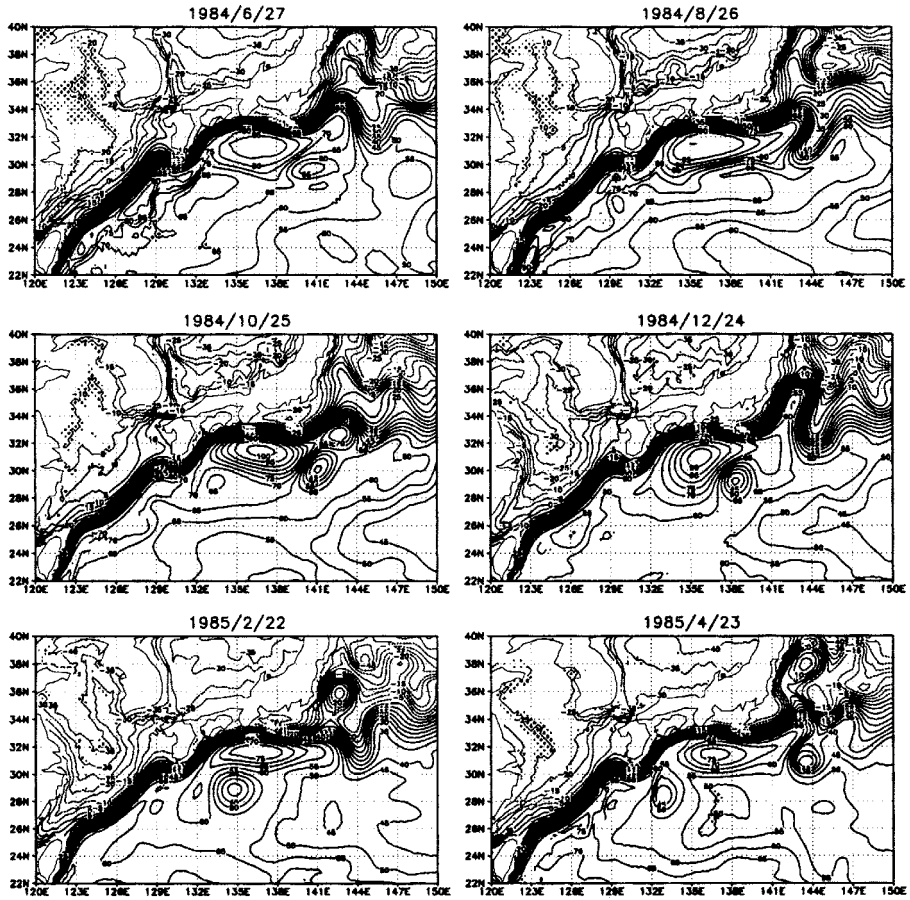


**Fig. 1.** Time sequence of the sea surface height field near Japan from June 1984 through April 1985. The contour interval is 5 cm.

period, we see that the stationary meander in the Kuroshio extension region (144°E-147°E, 31°N-34°N) gradually develops from April to September, and extends southward (Fig. 1). In September, the cold eddy is shed from the Kuroshio Extension. This ring-like cold eddy moves slowly to the south-west, and finally dissipates about 7 months later near the Kuroshio axis south of Kyushu. The cold eddies observed at other periods show almost the same life cycle although details are different. Therefore the OGCM result suggests that the instability of Kuroshio Extension is responsible for the generation of cold eddies. To understand the mechanism of this instability, we have analyzed energetics in a way similar to Masina *et al*. (1999). The energy transfer $N$ from mean kinetic energy to eddy kinetic energy, which denotes the barotropic instability exciting disturbances when the sign is positive, is expressed as in the following:

$$N' = -\left(\overline{u'u'}\frac{\partial \bar{u}}{\partial x} + \overline{u'v'}\left(\frac{\partial \bar{u}}{\partial y} + \frac{\partial \bar{v}}{\partial x}\right) + \overline{v'v'}\frac{\partial \bar{v}}{\partial y}\right) \quad (1)$$

where $u'$ and $v'$ are eastward and northward velocity, respectively. The overbar represents the time mean; the prime represents the fluctuation from the mean. Similarly, the energy transfer $A'$ from eddy potential energy to eddy kinetic energy, which means baroclinic inability exciting disturbances when the sign is positive, is described as in the following:

$$A' = -g\frac{\overline{u'\rho'}\frac{\partial \bar{\rho}}{\partial x} + \overline{u'\rho'}\frac{\partial \bar{\rho}}{\partial y}}{\frac{\partial \overline{\rho_R}}{\partial z}} \quad (2)$$

where $g$ is the acceleration due to gravity, $\rho'$ is the fluctuation in density, and $\rho_R$ is the reference potential density (Wells *et al*., 2000). The mean field is derived from April to September in 1984 (Fig. 2); we discuss deviations from this mean field. The zonal section of $N'$ and $A'$ at 34°N averaged for the period is shown in Fig. 3. At this latitude, the model Kuroshio shows the quasi-stationary meander as seen in Fig. 2. A large positive core of the $A'$ is seen between 142°E and 144°E when the stationary meander develops. The contribution from the positive $N'$ term is minor there; this means that the instability is mainly due to the baroclinic energy transfer rather than the

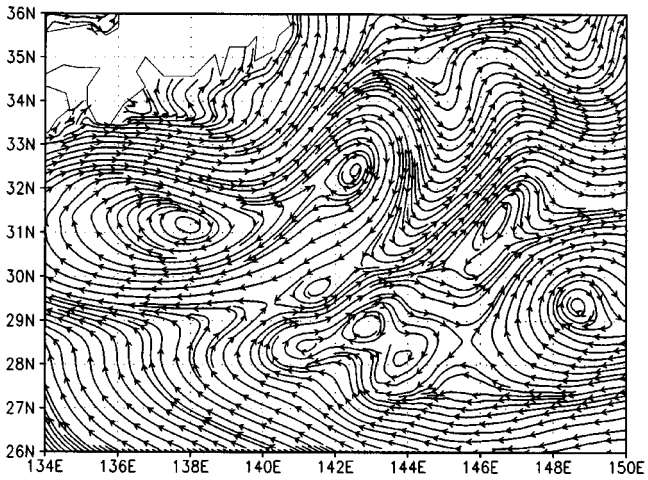


**Fig. 2.** Surface circulation averaged from April to September 1984.

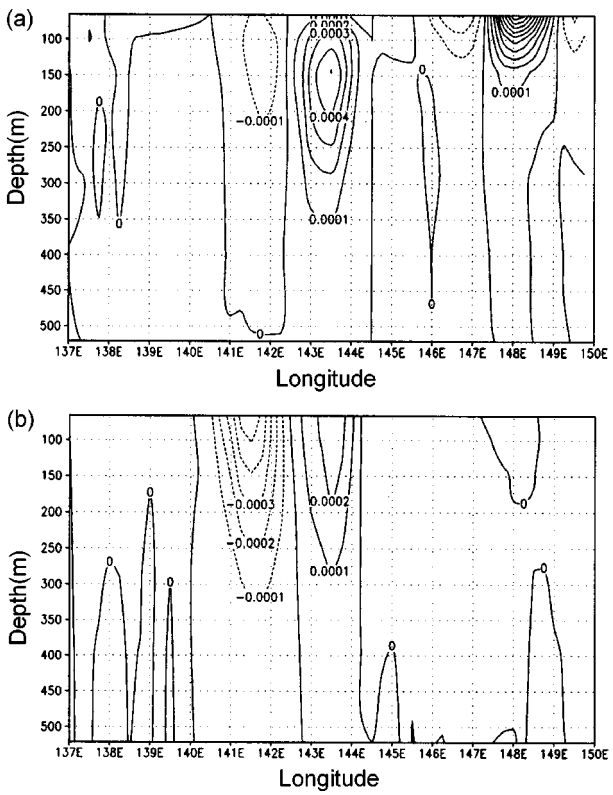


**Fig. 3.** Depth-longitude section at 34ºN: (a) A' ($cm^2s^{-3}$), (b) N' ($cm^2s^{-3}$). The contour interval is $5\times10^{-5}$ ($cm^2s^{-3}$).

barotropic energy transfer. Therefore, the quasi-stationary meander in this particular region of the Kuroshio Extension develops mainly owing to baroclinic instability and sheds a cold ring-like eddy.

**Warm Eddies:** We focus on the period of 1986-1987 when the positive anomaly of the streamfunction is seen in the west of the ridge (not shown). It is interesting to know how the warm eddy is related to the positive anomaly of the streamfunction. The positive anomaly of the streamfunction in the east of the ridge, which corresponds to the winter intensification of the western boundary current along the Izu-Ogasawara Ridge, is associated with the warm water piled up east of the ridge; this warm water intrudes into the Philippine Basin across the ridge, and propagates slowly with generating weak warm eddies in winter (Fig. 4). Thus the behavior of the warm eddies are different from the cold ring-like eddies generated from the Kuroshio Extension. The SSH anomaly field evolves consistently with the above view; the SSH anomaly accumulated near the Ridge by the end of winter propagates westward and generates positive height anomalies (not shown).

The positive anomaly of the streamfunction is associated with a deep current structure in the east of the ridge as seen in Fig. 5. However, west of the ridge, the anomalous velocity field is confined near the surface layer above a depth of 500 m. This suggests that the ridge contributes to the transformation of the barotropic motion into the surface-trapped baroclinic motion. Since the westward propagation speed of Rossby waves is so different between pure barotropic motion and the pure baroclinic motion, we somehow need strong vertical modal coupling in order to explain the slow westward propagation of the transport streamfunction anomaly west of the ridge (cf. Aiki and Yamagata, 2000). To understand this, we construct a simple model in the next section. As we have discussed so far, necessary elements to consider this problem are 1) baroclinicity of the ocean, 2) existence of the ridge, 3) nonlinearity of the momentum equation, and 4) basin-wide seasonal variations excited by winds.

## MODEL DESCRIPTION

The model developed here is a two-layer primitive ocean model with a submerged ridge as shown in Fig. 6 under the rigid lid approximation. The ridge mimics the Izu-Ogasawara Ridge and divides the model Philippine Basin in the west and the Pacific Basin in the east. We adopt this model to resolve the ocean variability of both the internal and external origins in the simplest way. The governing equations are written using the conventional notation as in the following:

$$\frac{\partial u_1}{\partial t} - q_1 v_1 h_1 + \frac{\partial K_1}{\partial x} = -\frac{1}{\rho_0}\frac{\partial P}{\partial x} + \frac{\tau^x}{\rho_0 h_1} + A_h \nabla^2 u_1 \qquad (3)$$

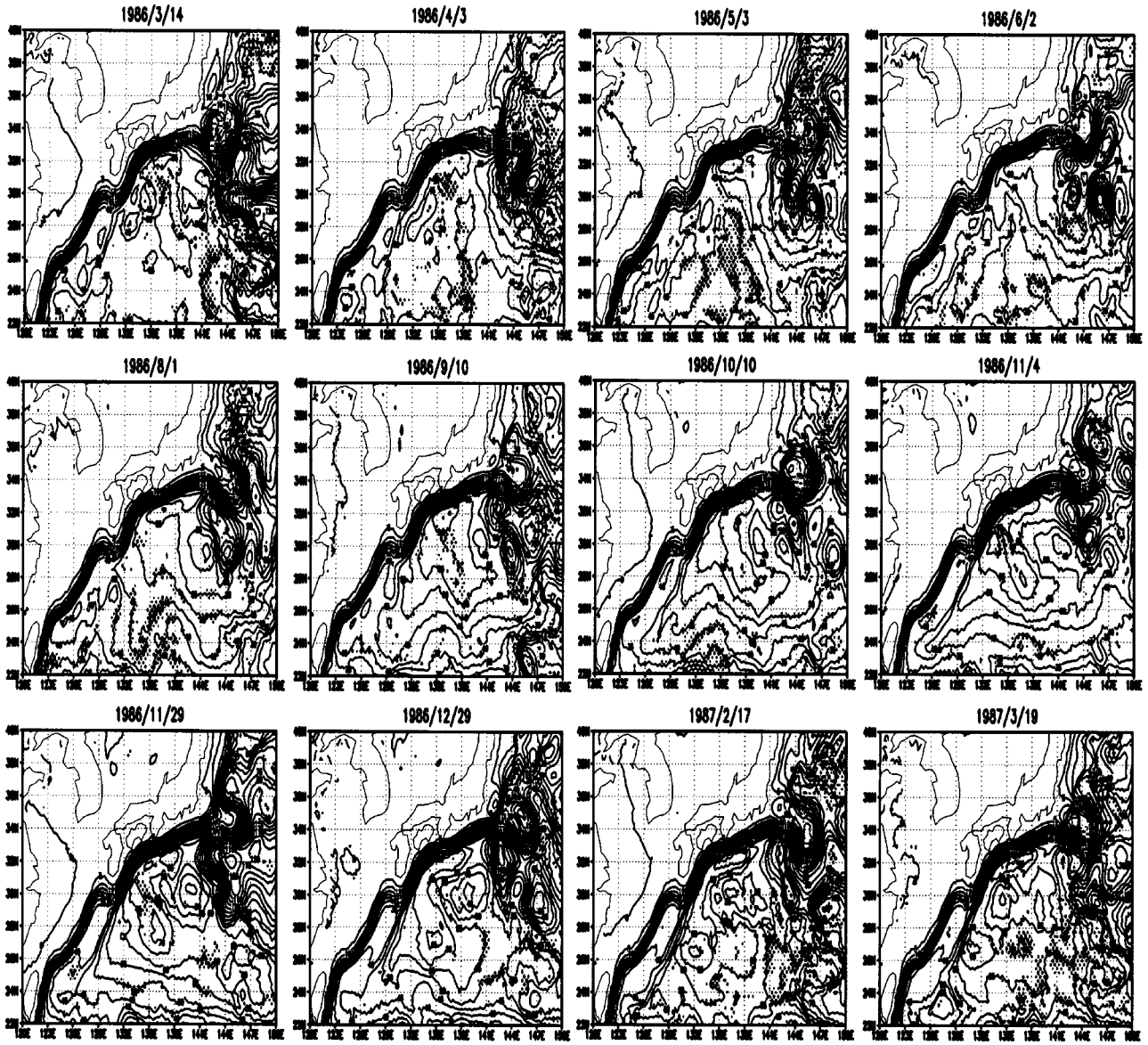


**Fig. 4.** Time sequence of the streamfunction field in the Kuroshio region (120°E–150°E, 10°N–40°N) from March 1986 to March 1987. Note that the western boundary current along the Izu-Ogasawara Ridge leaks out an anticyclonic gyre west of the Ridge in November. The contour interval is 5 Sv.

$$\frac{\partial u_1}{\partial t} - q_1 v_1 h_1 + \frac{\partial K_1}{\partial y} = -\frac{1}{\rho_0}\frac{\partial P}{\partial y} + \frac{\tau^y}{\rho_0 h_1} + A_h \nabla^2 v_1 \tag{4}$$

$$\frac{\partial h_1}{\partial t} + \frac{\partial u_1 h_1}{\partial x} + \frac{\partial v_1 h_1}{\partial y} = 0 \tag{5}$$

where

$$q_1 = \frac{\zeta_1 + f}{h_1}$$

$$K_1 = \frac{u_1^2 + v_1^2}{2}$$

for the upper layer, and

$$\frac{\partial u_2}{\partial t} - q_2 v_2 h_2 + \frac{\partial K_2}{\partial x} = -\frac{1}{\rho_0}\frac{\partial P}{\partial x} + g'\frac{\partial P}{\partial x} + A_h \nabla^2 u_2 \tag{6}$$

$$\frac{\partial u_2}{\partial t} + q_2 v_2 h_2 + \frac{\partial K_2}{\partial x} = -\frac{1}{\rho_0}\frac{\partial P}{\partial y} + g'\frac{\partial h_1}{\partial y} + A_h \nabla^2 v_2 \tag{7}$$

where

$$h_2 = \text{total depth} - h_1$$

$$q_2 = \frac{\zeta_2 + f}{h_2}$$

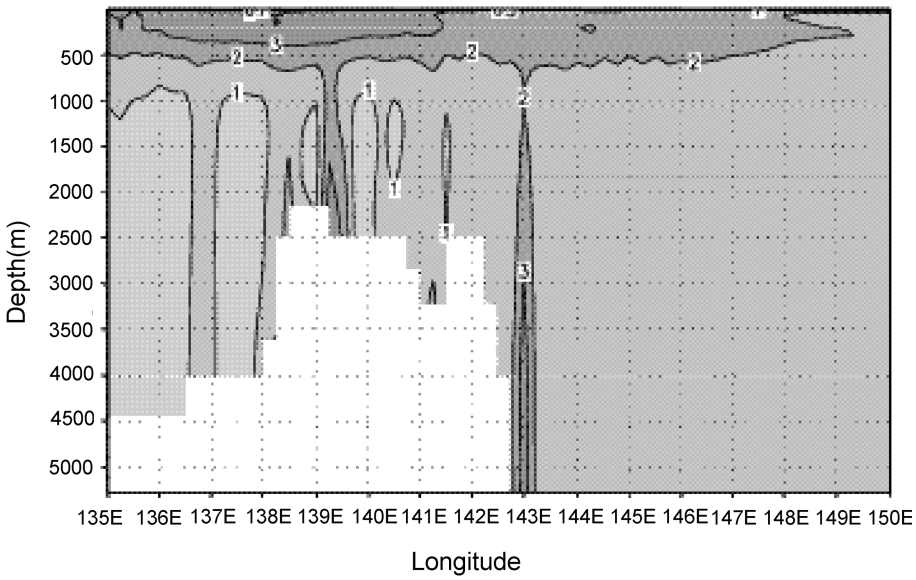


**Fig. 5.** Depth-latitude section of the root-mean-squared amplitude of the meridional velocity at 29°N. The contour interval is 1 $cms^{-1}$.

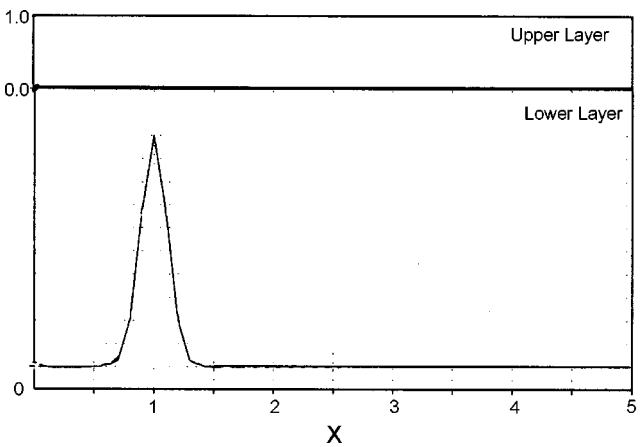


**Fig. 6.** The model ridge adopted in the present study. The total depth is 5000 m, and the zonal extent is 5000 km.

$$K_2 = \frac{u_2^2 + v_2^2}{2}$$

for the lower layer, where $q_i$ (i=1,2) are the potential vorticity defined in each layer on the beta-plane with a reference latitude at 25°N and $K_i$ (i=1,2) are the kinetic energy. The surface pressure (i.e. $P$) is calculated using the Poisson equation.

The model ocean is 5000 km wide in longitude and 3000 km wide in latitude; the horizontal grid spacing is 20 km. The eddy diffusivity $A_h$ is $6.6\times10^2$ $m^2/s$ and $g'$ is 0.019 $m/s^2$. The bottom topography is given by $H_r \exp\{-0.4\times((x\text{-}1000\text{ km})^2/W^2)\}$, where $H_r$ is the maximum height of the model ridge (2500 m), and W is the zonal extent of the ridge (900 km). We assume that the ridge is always submerged in the lower layer. Based on the observation, we have adopted the upper layer thickness of 1000 m and the lower layer thickness of 4000 m. The eastern and western boundaries are slippery, whereas the northern and southern boundaries are non-slippery. In particular, we have added a sponge layer along the southern boundary to dissipate artificial Kelvin waves.

As the forcing filed, we adopt the sinusoidal wind stress as in the following:

$$\tau^x = -Z\cos\left(\pi\frac{y}{L}\right) \tag{9}$$

where $Z$ = 0.4 $N/m^2$ and $L$ is the latitudinal extent of the basin. As seen in Eq. (9), only the zonal component of the wind stress is assumed for simplicity. The model is driven with this constant wind for 2500 days in order to spin up the ocean. Then we have changed the wind sinusoidally for 1980 days as in the following,

$$\tau^x = -Z\cos\left(\pi\frac{y}{L}\right)\times\left(1+\sin\left(2\pi\frac{t}{t_s}\right)\right)$$

where $t_s$ denotes the period of the seasonal wind change. This period corresponds to a model year and is 180 days in the present configuration.

We carry out three experiments called TA, NA, and NT. The experiment TA takes into account of both bottom topography and nonlinear advection. Another experiment NA neglects the nonlinear advection with retaining the bottom topography. The other experiment NT neglects the bottom topography, while keeping the nonlinear advection.

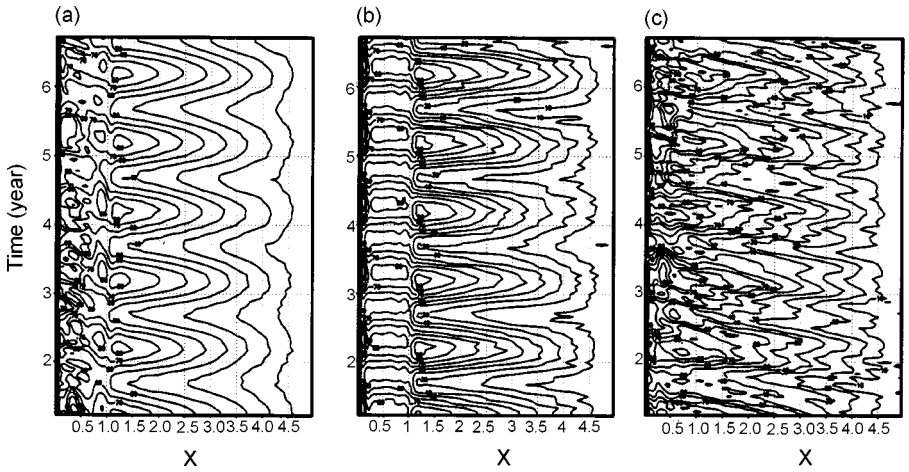


**Fig. 7.** Longitude-time section of the transport streamfunction at 27° N: (a) TA; (b) NA; (c) NT. The high-frequency variability is filtered out in TA and NT. The contour interval is 10 Sv.

## MODEL RESULTS

The model is driven for 1980 days (corresponding to 11 model years) after spin-up as described in Section 3. Hereafter we discuss the simulation results from the beginning of year 6 through the end of year11 for the three experiments TA, NA and NT. The longitude-time section of the total transport streamfunction at 27°N, in which the high-frequency internal variations in TA and NT are filtered out by introducing 90 days running-mean, is shown in Fig. 7 for each experiment. We note that low-frequency internal variations generated by eddy activities in the experiments including the nonlinear advection (TA, NT) are not removed.

The transport variation in the Pacific Basin shows a clear seasonal variation in association with the external winds in all three cases. A localized positive circulation locked to the seasonal cycle is found just east of the ridge in TA. This secondary circulation pattern appears to propagate slowly westward in the Philippine Basin in contrast to the quasi-periodic oscillation in the Pacific Basin. The slow propagation gives rise to a phase lag in the seasonal transport variation of the western boundary current in the Philippine Basin compared to that of the quasi-steady Sverdrup transport variation in the Pacific Basin, as we will see later. Examining the plan view of the streamfunction field, we find that this secondary positive circulation change in the east of the ridge is related to westward shedding of warm eddies near the Kuroshio Extension region; this warm eddy shedding is active in winter. In summer, on the other hand, we find cold eddies shed from the ridge; the cold eddies are associated with the negative (cyclonic) circulation.

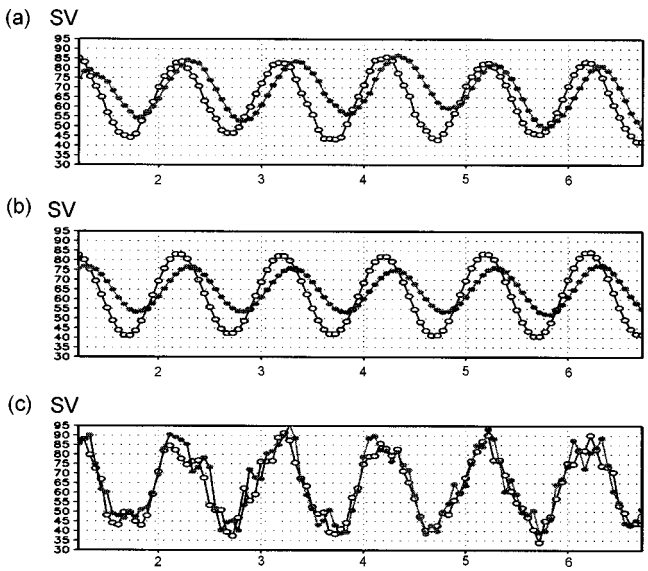


**Fig. 8.** Time series of the transport streamfunction near the ridge. White circles represent values east of the ridge (X=1.15, Y=1.7), whereas black circles represent values west of the ridge (X=0.85, Y=1.7). (a) TA; (b) NA; (c) NT.

The time variation in transport of the western boundary current across 27°N in the model basin is shown in Fig. 8. A remarkable feature is the existence of the phase lag of the transport maximum in TA and NA in which topography is included. In both cases, the peak transport in the Philippine Basin occurs about two months after the peak of the Sverdrup transport in the Pacific Basin. This suggests that the inclusion of topography can introduce another phase lag in response to winds even without nonlinearity. We will show that this is due to the joint effect of baroclinicity and bottom topography (JEBAR).

In the linear case (NA), the magnitude of the sea-

sonal variation of the transport is reduced in the Philippine Basin partly because of the blocking effect of the ridge; the maximum is reduced and the minimum is increased. However, the case for TA only shows the increase of the minimum; the maximum is almost the same. This asymmetry is due to existence of nonlinearity in the momentum equation. In other words, the anticyclonic circulation generated near the ridge lessens the blocking effect of the ridge.

As seen in the longitude-time section for the upper layer thickness (not shown), pure baroclinic long Rossby waves are shed regularly through the seasonal adjustment process at the eastern boundary (Anderson and Killworth, 1979). However, those waves steepen owing to their nondispersive property and break into mesoscale eddies with the barotropic component near caustics in the central part of the Pacific Basin. Because of this, the upper layer thickness in the central Pacific Basin changes simultaneously in accord to the annual variation of winds. The longitude-time section for the transport streamfunction cannot capture those variations mostly reflected in the baroclinic field in the Pacific Basin.

As we discussed using the total transport streamfunction field, only in the experiment including the bottom topography and advection, i.e., TA, warm and cold eddies associated with variations of the upper layer thickness are generated near the ridge and propagate westward a little faster than the baroclinic long Rossby wave speed. This increase of the propagation speed may be explained by the coupling between the baroclinic motion and the barotropic motion due to nonlinearity (cf. Aiki and Yamagata, 2000). This is because the eddies generated near the ridge are surface-intensified as seen in the meridional velocity field (Fig. 9). The surface-intensified eddies are also clearly seen in the upper-layer thickness field (not shown). The eddy generation is locked to the annual variation in the Pacific Basin; cold eddies are shed from the Kuroshio Extension in summer and the warm eddies are generated by the positive anomaly accumulated near the ridge. This generation process simulated by the present simple model is quite similar to the OGCM results.

## SUMMARY AND DISCUSSION

Using OGCM results and a simple two-layer model with a ridge, we have tried to understand the seasonal generation of cold and warm eddies south of Japan. The analysis of the OGCM data shows that the ring-like cold baroclinic eddies associated with cyclonic circulation are shed from late summer to early fall from the Kuroshio Extension east of the Izu-Ogasawara Ridge owing to baroclinic instability. On the other hand, the warm baroclinic eddies are generated by the positive warm water anomaly accumulated near the Ridge in winter, which corresponds to the basin-wide intensification of the wind-driven Sverdrup transport in winter. We are successful in reproducing the behavior of those eddies using a simple two-layer primitive equation model driven by

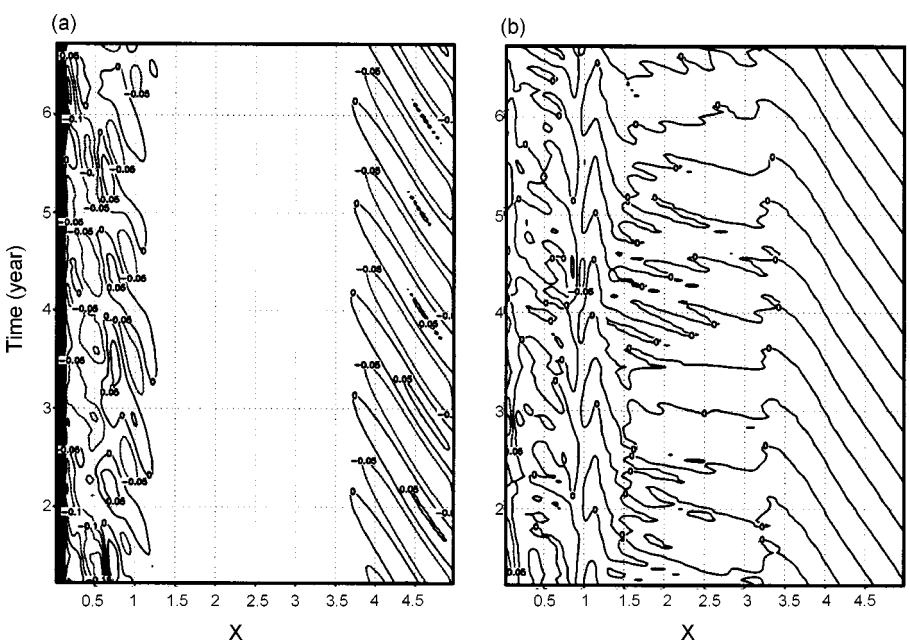


**Fig. 9.** Longitude-time section of the meridional velocity at 27°N for TA. (a) upper layer; (b) lower layer. The contour interval is 0.05 cm.

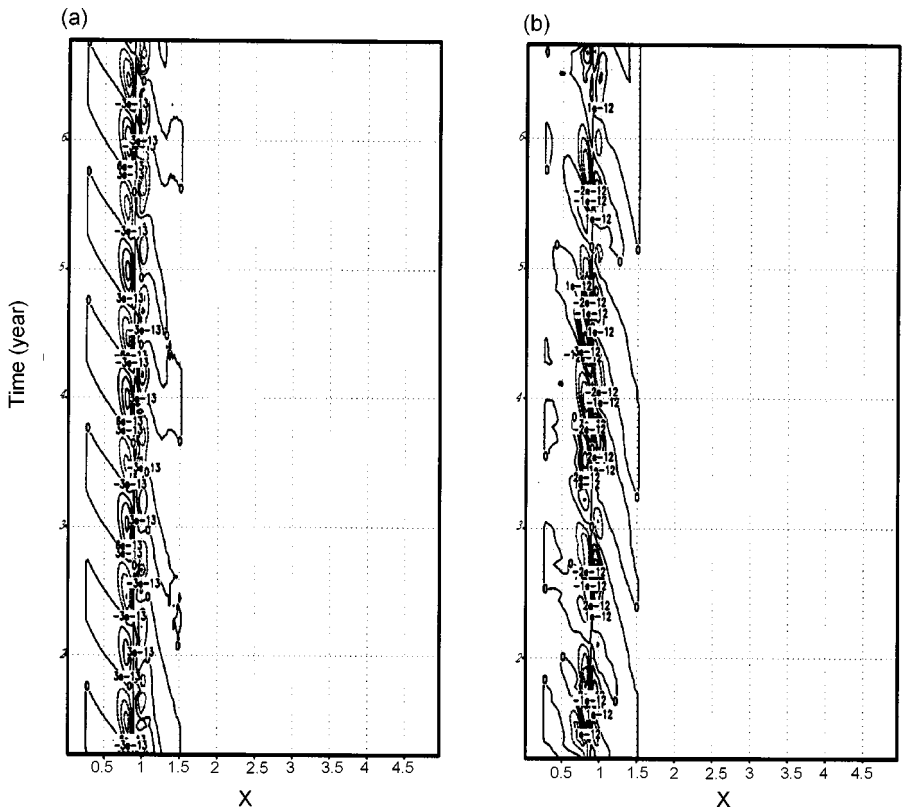


**Fig. 10.** Longitude-time section of JEBAR at 27°N. (a) NA; (b) TA. The contour interval is $2\times10^{-13}s^{-2}$.

time-varying winds. Those eddies carry the basin-wide barotropic seasonal signals quite slowly west of the ridge; this introduces a phase lag in the timing of the maximum transport in the sub-basin west of the ridge. It is demonstrated that the existence of bottom topography (the ridge), baroclinicity (two-layer), and nonlinearity due to advection are three necessary elements for the generation of these eddies south of Japan.

Since the interaction between baroclinicity and bottom topography is understood succinctly in terms of the concept of JEBAR (joint effect of baroclinicity and bottom topography) introduced by Sarkisyan and Ivanov (1971) (see Appendix), it will be of interest to show the longitude-time variation of the term (Fig. 10) as in Sakamoto and Yamagata (1996). The JEBAR certainly lessens the role of winds from fall to winter; it is just like adding the extra positive wind stress curl which is localized near the edge. From spring to summer, on the other hand, the JEBAR strengthens the role of winds by adding the virtual negative wind stress curl near the edge. In this way, it also introduces a phase lag in the transport streamfunction across the ridge. Because the synoptic eddy formation comes into play owing to nonlinearity in the momentum equation, the role of JEBAR is not so simple as compared to the linear model result of Sakamoto and Yamagata (1996) developed in a somewhat different context. However, Fig. 10 certainly captures the importance of JEBAR to understand the interaction between localized topography and baroclinicity.

As suggested by various model and observational results shown in the introduction, the baroclinic eddies south of Japan appear to play important roles on generating the Kuroshio variability. The present work suggests that those baroclinic eddies may be generated owing to nonlinearity through the interaction between the basin-wide response to seasonal winds and the localized bottom topography such as the Izu-Ogasawara Ridge. We believe that this possible link between the eddy generation and the seasonal variation will shed new light on the predictability study on the Kuroshio meandering.

## ACKNOWLEDGEMENTS

This research was supported by CREST of JST (Japanese Science and Technology Cooperation) and by Ministry of Education, Science, Sports and Culture, Japan under the grant of scientific research of priority area (B).

## APPENDIX

Neglecting the time derivative terms and diffusion terms of Eqs. (3), (4), (6), and (7), and adding

$$A^x + B^x = -\frac{H}{\rho_0}\frac{\partial(P_b - \rho_2 gH)}{\partial x} + \frac{\tau^x}{\rho_0} - g' h_1 \frac{\partial h_1}{\partial x} \quad \text{(A1)}$$

$$A^y + B^y = -\frac{H}{\rho_0}\frac{\partial(P_b - \rho_2 gH)}{\partial y} + \frac{\tau^y}{\rho_0} - g' h_1 \frac{\partial h_1}{\partial y} \quad \text{(A2)}$$

the upper-layer equations multiplied by $h_1$ to the lower-layer equations multiplied by $h_2$, we obtain where

$$A^x = -q_1 v_1 h_1^2 - q_2 v_2 h_2^2,\ B^x = h_1 \frac{\partial K_1}{\partial x} + h_2 \frac{\partial K_2}{\partial x}$$

$$A^y = -q_1 v_1 h_1^2 - q_2 v_2 h_2^2,\ B^y = h_1 \frac{\partial K_1}{\partial y} + h_2 \frac{\partial K_2}{\partial y}$$

Here we have introduced the total depth $H=h_1+h_2$ and the bottom pressure $P_b=P+g(\rho_1 h_1+\rho_2 h_2)$. Dividing above equations by $H$ and taking the curl afterward, we obtain the torque balance in the following:

$$curl\left(\frac{A+B}{H}\right) = J\left(\frac{g'}{2}h_1^2, \frac{1}{H}\right) + \frac{1}{\rho_0} curl\frac{\tau}{H} \quad \text{(A3)}$$

In the above balance, the first term of the right hand side is called the JEBAR term that plays a role similar to the second term due to the wind action in the torque balance (Greatbatch *et al*., 1991; Sakamoto and Yamagata, 1996). When the JEBAR is positive (negative), it tends to strengthen the anticyclonic (cyclonic) circulation.

## REFERENCES


Aiki, H. and Yamagata, T., 2000. "Successive formation of planetary lenses in an intermediate layer" *Geophys. Astrophys. Fluid Dynamics*, **92**: 1–29.

Anderson, D.L.T. and Killworth, P.D., 1979. "Non-linear propagation of long Rossby waves" *Deep-Sea Res.*, **26A**: 1033–1050.

Ebuchi, N. and Hanawa, K., 2000. "Mesoscale eddies observed by TOLEX-ADCP and TOPEX/POSEIDON altimeter in the Kuroshio recirculation region south of Japan" *J. of Oceanogr.*, **56**: 43.

Endoh, T. and Hibiya, T., 2001. "Numerical simulation of the transient response of the Kuroshio leading to the large meander formation south of Japan" *J. Phys. Oceanogr.* (in press).

Gill, A.E., 1982. Atmosphere-Ocean Dynamics, *Academic Press*, International geophysics series **30**: 662.

Greatbatch, R.J., Fanning, A.F., Goulding, A.D. and Levitus, S., 1991. "A diagnosis of interpentadal circulation changes in the North Atlantic" *J.Geophys.Res.*, **96**: 22009–22023.

Kagimoto, T., 1999. "Numerical study on transport Variations of Kuroshio" Doctral Dissertation, The University of Tokyo.

Kawabe, M., 1995. "Variation of current path, velocity, and transport of the Kuroshio in relation with the large meander" *J. Phys. Oceanogr.*, **25**: 3103–3117.

Killworth, P.D., 1987. "Topographic instabilities in level model OGCMs" *Ocean modeling*, **75**: 9–12.

Levitus, S. and Boyer, T.P., 1994. "World Ocean Atlas. Vol. 4: Temperature" *NOAA Atlas NESDIS 4, U. S. Govt. printing Office*, pp. 117.

Levitus, S., Burgett, R. and Boyer, T.P., 1994. "World Ocean Atlas. Vol.5: Salinity" *NOAA Atlas NESDIS 3, U. S. Govt. printing Office*, pp. 99.

Masina, S., Philander, S.G.H. and Bush, A.B.G., 1999. "An analysis of tropical instability waves in a numerical model of the Pacific Ocean 2. Generation and energetics of the waves" *J. Geophys. Res.*, **104**: 29637–29661.

Miyazawa, Y., Guo, X., Hukuda, H. and Yamagata, T., 2000. "Eddy resolving Kuroshio simulation: Kuroshio path variation" manuscript in preparation.

Pacanowski, R.C., 1996. "MOM2 documentation, user's guide and reference manual" *GFDL Ocean Tech. Rep. 3.1*, Geophysical Fluid Dynamics laboratory/NOAA [Available from GFDL, Princeton University, Princeton, NJ 08542].

Pacanowski, R.C. and Philander, S.G.H., 1981. "Parameterization of vertical mixing in numerical models of tropical oceans" *J. Phys. Oceanogr.*, **11**: 1443–1451.

Rosati, A. and Miyakoda, K., 1988. "A general circulation model for upper ocean simulation" *J. Phys. Oceanogr.*, **18**, 1601–1626.

Sakamoto, T. and Yamagata, T., 1996. "Seasonal transport variations of the wind-driven ocean circulation in a two-layer planetary geostrophic model with a continental slope" *J. Marine Res.*, **54**: 261–284.

Sarkisyan, A.S. and Ivanov, V.F., 1971. "Joint effect of baroclinicity and bottom relief as an important factor in the dynamics of sea currents" *Izv.Acad.Sci.USSR Atom.Oceanic.Phys.*, **7**: 173–188.

Smagorinsky, J., 1963. "General circulation experiments with the primitive equations. I. The basic experiment" *Mon. Wea. Rev.*, **91**: 99–164.

Smith, T.M., Reynolds, R.W., Livezey, R.E. and Stokes, D.C., 1996. "Reconstruction of historical sea surface temperature using empirical orthogonal function" *J. Climate*, **9**: 1403–1420.

Waseda, T., Mitsudera, H., Taguchi, B. and Yoshikawa, Y., 2000. "On the eddy-Kuroshio interaction: initialization and evolution of meso-scale eddy" *J. Phys. Oceanogr.* (submitted).

Wells, N.C., Vchenko, V.O. and Best, S.E., 2000. "Instabilities in the Agulhas retroflection current system: a comparative model study" *J. Geophys. Res.*, **105**, 3233–3241.